

Quantum Phase Transition and Universal Dynamics in the Rabi model

Myung-Joong Hwang, Ricardo Puebla, Martin B. Plenio

Institut für Theoretische Physik and IQST, Albert-Einstein-Allee 11, Universität Ulm, D-89069 Ulm, Germany

(Dated: March 18, 2022)

We consider the Rabi Hamiltonian which exhibits a quantum phase transition (QPT) despite consisting only of a single-mode cavity field and a two-level atom. We prove QPT by deriving an exact solution in the limit where the atomic transition frequency in unit of the cavity frequency tends to infinity. The effect of a finite transition frequency is studied by analytically calculating finite-frequency scaling exponents as well as performing a numerically exact diagonalization. Going beyond this equilibrium QPT setting, we prove that the dynamics under slow quenches in the vicinity of the critical point is universal, that is, the dynamics is completely characterized by critical exponents. Our analysis demonstrates that the Kibble-Zurek mechanism can precisely predict the universal scaling of residual energy for a model without spatial degrees of freedom. Moreover, we find that the onset of the universal dynamics can be observed even with a finite transition frequency.

Introduction.— Universality plays a key role for our understanding of quantum phase transitions (QPT) in interacting quantum systems [1]. While the concept of universality is well-established in equilibrium QPT, the question to what extent the concept of universality could be extended to non-equilibrium dynamics of QPT remains largely to be explored [2, 3]. For a slow quench across a QPT, the closing spectral gap at a critical point leads to a breakdown of the adiabaticity regardless of the quench rate. The scaling of defect formation has been shown to be entirely controlled by critical exponents and quench rate through a successful application of the Kibble-Zurek mechanism (KZM) [4–7], originally developed for classical phase transitions, to QPT in short-range interaction models [8–12]. However, whether this scaling holds for fully-connected models [13], which lack spatial degrees of freedom, such as Dicke [14] or Lipkin-Meshkov-Glick (LMG) model [15] remains an open problem [16, 17].

The Dicke model considers a system of a quantized single-mode cavity field uniformly coupled to N two-level atoms. It exhibits a superradiant QPT in the thermodynamic limit ($N \rightarrow \infty$) [18–21]. While tremendous efforts have been devoted to understand the QPT of the Dicke model both in and out of equilibrium [18–26], a criticality of the Rabi model [26–31], the most simplified version of Dicke model with $N = 1$, has been hitherto largely overlooked. Having only two constituent particles, the Rabi model is far from being in the thermodynamic limit where a QPT typically occurs; however, a ratio of the atomic transition frequency Ω to the cavity field frequency ω_0 that approaches infinity, $\Omega/\omega_0 \rightarrow \infty$, can play the role of a thermodynamic limit [26] that allows the spectral gap to be precisely closed at the critical point [1].

In this letter, we firstly establish the theory of equilibrium QPT of the Rabi model. At the core of our analysis is a low-energy effective Hamiltonian that is valid for $\Omega/\omega_0 \gg 1$ and becomes exact in the $\Omega/\omega_0 \rightarrow \infty$ limit. We derive an exact solution for eigenstates, an energy spectrum, expectation values of relevant observables, and critical exponents in the $\Omega/\omega_0 \rightarrow \infty$ limit. Our solution shows that there exists a critical atom-cavity coupling strength g_c beyond which the Z_2 parity symmetry is broken and the cavity field is macroscop-

ically occupied. Further, the effect of a finite value of Ω/ω_0 on the QPT is analyzed in the spirit of the finite-size scaling analysis. The leading order corrections to the ground state energy, the excitation energy, the average photon number, and the variance of cavity field quadratures at the critical point are derived analytically, from which *finite-frequency* scaling exponents are obtained. We also perform an exact diagonalization and find an excellent agreement with analytical results.

Our establishment of the equilibrium QPT allows us to investigate the universality in the dynamics of the Rabi model. Particularly, we are interested in quench dynamics where the system is initially prepared in the ground state and the control parameter g is tuned towards to the critical point linearly in time with a quench time τ_q starting from $g = 0$ [8–11, 32–34]. On the one hand, we solve the dynamics exactly in the $\Omega/\omega_0 \rightarrow \infty$ limit, and calculate the residual energy as a measure of the degree of non-adiabaticity, which shows a power-law scaling with the quench time τ_q . On the other hand, we obtain such a scaling solely from the critical exponents found in the first part of the letter. To this end, we apply KZM to the adiabatic perturbation theory [9, 32–34] and the dynamical critical function method [17], independently. Both approaches give rise to the same universal scaling that precisely predicts the exact dynamics, demonstrating that the KZM can lead to a universal dynamics for a fully-connected model.

Finally, we consider the same quench dynamics with a finite value of Ω/ω_0 , and show that, as one decreases the ratio Ω/ω_0 , there is a crossover from the universal scaling to the τ_q^{-2} scaling, a typical scaling of the adiabatic dynamics with a finite quench time for a gapped system [16, 32, 33]. We identify a range of quench times which leads to dynamics that closely follows the universal scaling, and show that the onset of the universal dynamics can be observed for a finite Ω/ω_0 . The crossover from the universal to the τ_q^{-2} scaling is also observed in the $\Omega/\omega_0 \rightarrow \infty$ limit by ending the quench of the control parameter g below the critical point. It demonstrates that the spectral gap opening due to finite Ω/ω_0 has the same effect as ending the quench below the critical point in the $\Omega/\omega_0 \rightarrow \infty$ limit.

Quantum phase transition.— We consider the Rabi Hamil-

tonian,

$$H_{\text{Rabi}} = \omega_0 a^\dagger a + \frac{\Omega}{2} \sigma_z - \lambda(a + a^\dagger) \sigma_x \quad (1)$$

where $\sigma_{x,z}$ are Pauli matrices for a two-level atom and a (a^\dagger) is an annihilation (creation) operator for a cavity field. The cavity field frequency is ω_0 , the transition frequency Ω , and the coupling strength λ . We denote $|\uparrow$ ($|\downarrow$) as eigenstates of σ_z , and $|m\rangle$ the eigenstate of $a^\dagger a$. The parity operator, $\Pi = e^{i\pi(a^\dagger a + \frac{1}{2}(1 + \sigma_z))}$, which measures an even-odd parity of total excitation number, commutes with H_{Rabi} . The Z_2 parity symmetry has been shown to be sufficient for the model to be integrable [35]; however, a lack of a closed form solution makes the approach in Ref. [35] not directly applicable to investigate the QPT.

Note that, in the $\Omega/\omega_0 \rightarrow \infty$ limit, the low-energy physics of H_{Rabi} would be confined in the subspace \mathcal{H}_\downarrow for $\lambda/\Omega \ll 1$. Thus, we use the Schrieffer-Wolff (SW) transformation [36, 37] to derive a low-energy effective Hamiltonian. Namely, we firstly find a unitary transformation $U = \exp[\frac{\lambda}{\Omega}(a + a^\dagger)(\sigma_+ - \sigma_-)]$, which decouples the \mathcal{H}_\downarrow and \mathcal{H}_\uparrow subspaces up to second order in λ/Ω , and then project onto \mathcal{H}_\downarrow , i.e., $H_{np} \equiv \langle \downarrow | U^\dagger H_{\text{Rabi}} U | \downarrow \rangle$, which reads

$$H_{np} = \omega_0 a^\dagger a - \frac{\omega_0 g^2}{4} (a + a^\dagger)^2 - \frac{\Omega}{2} + \mathcal{O}\left(\frac{g^3 \omega_0^{3/2}}{\Omega^{1/2}}\right), \quad (2)$$

where $g = 2\lambda/\sqrt{\omega_0 \Omega}$ [38]. Eq. (2) can be diagonalized to give $H_{np} = \epsilon_{np} b^\dagger b - \Omega/2$ with $\epsilon_{np} = \omega_0 \sqrt{1 - g^2}$, which is real only for $g \leq 1$ and vanishes at $g = 1$, locating the QPT. The low-energy eigenstates of H_{Rabi} for $g \leq 1$ are $|\phi_{np}^m(g)\rangle = \mathcal{S}[r_{np}(g)] |m\rangle |\downarrow\rangle$ with $\mathcal{S}[x] = \exp[\frac{x}{2}(a^{\dagger 2} - a^2)]$ and $r_{np}(g) = -\frac{1}{4} \ln(1 - g^2)$.

The failure of Eq. (2) for $g > 1$ suggests that the number of photons occupied in the cavity field becomes proportional to Ω/ω_0 so that the higher order terms cannot be neglected, i.e., *superradiance* occurs; it also suggests that \mathcal{P}_\downarrow is no longer the low-energy subspace. In order to properly capture the low-energy physics, we transform H_{Rabi} of Eq. (1) by displacing the cavity field a , i.e., $\tilde{H}_{\text{Rabi}}(\pm\alpha_g) = \mathcal{D}^\dagger[\pm\alpha_g] H_{\text{Rabi}} \mathcal{D}[\pm\alpha_g]$ with $\mathcal{D}[\alpha] = e^{\alpha(a^\dagger - a)}$ and $\alpha_g = \sqrt{\frac{\Omega}{4g^2 \omega_0}}(g^4 - 1)$, which reads

$$\tilde{H}_{\text{Rabi}}(\pm\alpha_g) = \omega_0 a^\dagger a + \frac{\tilde{\Omega}}{2} \tau_z^\pm - \tilde{\lambda}(a + a^\dagger) \tau_x^\pm \quad (3)$$

where $\tau_z^\pm \equiv |\uparrow^\pm\rangle \langle \uparrow^\pm| - |\downarrow^\pm\rangle \langle \downarrow^\pm|$ ($|\downarrow^\pm\rangle = \frac{\Omega}{2\tilde{\Omega}} \sigma_z \pm \frac{2\lambda\alpha_g}{\tilde{\Omega}} \sigma_x$). Eq. (3) has the same structure as Eq. (1) with rescaled frequencies $\tilde{\lambda} = \frac{\sqrt{\omega_0 \Omega}}{2g}$ and $\tilde{\Omega} = g^2 \Omega$. Importantly, the rescaled frequencies satisfy $\tilde{\lambda}/\tilde{\Omega} \ll 1$ for $g > 1$, indicating that the low-energy physics is confined in $\mathcal{H}_{\downarrow^\pm}$. Now, we apply the SW transformation to Eq. (3) and find

$$H_{sp} = \omega_0 a^\dagger a - \frac{\omega_0}{4g^4} (a + a^\dagger)^2 - \frac{\Omega}{4} (g^2 + g^{-2}) + \mathcal{O}\left(\frac{\omega_0^{3/2}}{g^7 \Omega^{1/2}}\right), \quad (4)$$

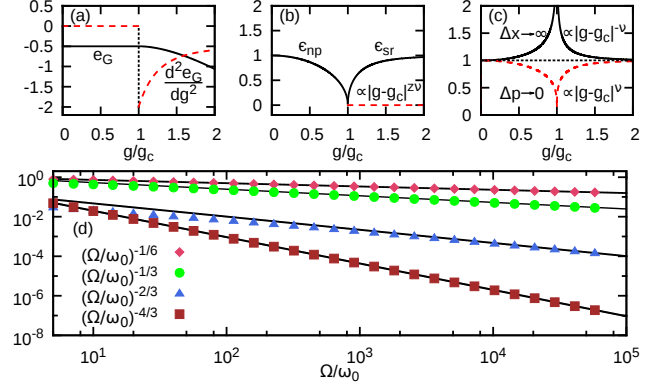


FIG. 1. Top panel: exact solutions of the Rabi model in the $\Omega/\omega_0 \rightarrow \infty$ limit as a function of the dimensionless coupling strength g/g_c for (a) the rescaled ground state energy e_G (solid) and $d^2 e_G/d^2 g$ (red-dashed), (b) the excitation energy ϵ (solid) and the energy difference between the ground and the first excited state (red-dashed) showing the ground state degeneracy for $g/g_c \geq 1$, and (c) the variance of position Δx (solid) and momentum Δp (red-dashed) quadrature of the cavity field, and $\Delta x \Delta p$ (dotted). In (b) and (c), the scaling relation near the critical point is indicated. Bottom panel: a leading order correction for finite Ω/ω_0 at $g = g_c$ for Δp , ϵ , the order parameter n_c , and e_G from top to bottom, respectively. The analytical results (lines) predict precisely the exact diagonalization results (points) for all observables. The finite-frequency scaling exponents for each observable are indicated.

whose excitation energy is found to be $\epsilon_{sp} = \omega_0 \sqrt{1 - g^{-4}}$, which is real for $g > 1$. Note that two independent choices of $\alpha = \pm\alpha_g$ in Eq. (3) lead to an identical spectrum. The low-energy eigenstates of H_{Rabi} for $g > 1$, $|\phi_{sp}^m(g)\rangle_\pm = \mathcal{D}[\pm\alpha_g] \mathcal{S}[r_{sp}(g)] |m\rangle |\downarrow^\pm\rangle$ where $r_{sp}(g) = -\frac{1}{4} \ln(1 - g^{-4})$, are, therefore, degenerate; they also have a spontaneously broken parity symmetry, as evident from the non-zero coherence of the field $\langle a \rangle = \pm\alpha_g$. The higher order corrections in Eq. (2) and (4) vanish exactly in the $\Omega/\omega_0 \rightarrow \infty$ limit. Therefore, H_{np} and H_{sp} are the *exact* low-energy effective Hamiltonian for the *normal phase* ($g < 1$) and *superradiant phase* ($g > 1$), respectively, for which the subscripts *np* and *sp* stand. See Ref. [39] for a detailed derivation of the effective Hamiltonian and its solution.

Our exact solution shows that the superradiant QPT occurs at the critical point $g_c = 1$. The rescaled cavity photon number $n_c = \frac{\omega_0}{\Omega} \langle a^\dagger a \rangle$ is zero for $g < g_c$ and $n_c = (g^4 - g_c^4)/4g^2$ for $g > g_c$; thus, n_c is an order parameter. The rescaled ground state energy, $e_G(g) \equiv \frac{\omega_0}{\Omega} E_G(g)$ is $-\omega_0/2$ for $g < g_c$ and $-\omega_0(g^2 + g^{-2})/4$ for $g > g_c$. While $e_G(g)$ is continuous, $d^2 e_G(g)/d^2 g$ is discontinuous at $g = g_c$, revealing the second-order nature of the QPT [Fig. 1 (a)]. Near the critical point, the excitation energy in both phases, ϵ_{np} and ϵ_{sp} , vanishes as $\epsilon(g) \propto |g - g_c|^{z\nu}$ with $z\nu = 1/2$ [Fig. 1 (b)], where ν is the critical exponent and z is the dynamic critical exponent [1]. Meanwhile, the variance of position quadrature of the field $x = a + a^\dagger$, which we identify as a characteris-

tic length scale, diverges as $\Delta x(g) \propto |g - g_c|^{-\nu} \propto \epsilon^{-z}$, from which we find that $z = 2$ and $\nu = 1/4$ [Fig. 1 (c)]. The critical point also accompanies an infinite amount of squeezing in the momentum quadrature $p = i(a^\dagger - a)$ so that it remains in the minimum uncertainty state for any g , i.e., $\Delta x(g)\Delta p(g) = 1$ [Fig. 1 (c)].

Finite-frequency scaling.— We complete our study of the equilibrium QPT by investigating the *finite-frequency* effect. Firstly, we derive a leading order correction to the exact effective Hamiltonian. To this end, we find a unitary transformation $U^\Omega = \exp[\frac{\lambda}{\Omega}(a + a^\dagger) + \frac{4\lambda^3}{3\Omega^3}(a + a^\dagger)^3(\sigma_+ - \sigma_-)]$ of Eq. (1) that decouples the \mathcal{H}_\downarrow and \mathcal{H}_\uparrow subspaces up to *fourth* order in λ/Ω and project to \mathcal{H}_\downarrow to obtain [39]

$$H_{np}^\Omega = H_{np} + \frac{g^4\omega_0^2}{16\Omega}(a + a^\dagger)^4 + \frac{g^2\omega_0^2}{4\Omega}, \quad (5)$$

where the leading order correction adds a quartic potential for the cavity field. Although H_{np}^Ω is not exactly solvable, a variational method can be used to derive analytical expectation values [39]. We find that, at the critical point, the excitation energy vanishes and the characteristic length scale diverges with a power-law scaling,

$$\epsilon_{g_c}(\Omega/\omega_0) = \omega_0 \left(\frac{2\Omega}{3\omega_0}\right)^{-1/3}, \quad \Delta x_{g_c}(\Omega/\omega_0) = \left(\frac{2\Omega}{3\omega_0}\right)^{1/6}. \quad (6)$$

In addition, the leading order correction for e_G and n_c are given by $e_{G,g_c}(\Omega/\omega_0) = (\omega_0/4)(2\Omega/3\omega_0)^{-4/3}$ and $n_{c,g_c}(\Omega/\omega_0) = 1/6(2\Omega/3\omega_0)^{-2/3}$. The exponents of these scaling relations, the finite-frequency scaling exponents, are found to be the same as the finite-size scaling exponents of corresponding observable for the Dicke model [40] and LMG model [41, 42], which also have the same critical exponent z and ν . We perform an exact diagonalization of Eq. (1) and show that the numerically obtained scaling exponents precisely match the analytical results [Fig. 1 (d)].

Universal scaling for adiabatic dynamics.— Having established the equilibrium QPT of the model, we are now able to investigate the dynamics of the QPT. We consider a protocol where the control parameter g is changed linearly in time, $g(t) = g_f t/\tau_q$, with g_f being the final value. The system is initially in the ground state. As $g(t)$ approaches the critical point, the vanishing spectral gap makes the relaxation time of the system diverge, inevitably creating quasiparticle excitations irrespective of how large the quench time τ_q is. Applying KZM [2, 4–11], we define a time instant \hat{t} that divides the dynamics into the adiabatic and impulsive regime from $\eta^2(t) = \dot{\eta}(t)$, where the accessible energy gap η is given as $\eta = 2\epsilon_{np}$ for $g < g_c$ due to the parity symmetry. From $\epsilon_{np} = \omega_0\sqrt{1 - g^2}$, we find $\hat{g} \sim g_c - (4\sqrt{2}\omega_0\tau_q)^{-\frac{1}{z\nu+1}}$ where the coupling instant $\hat{g} \equiv g(t = \hat{t})$ moves away from the critical point as one decreases the quench time so that the impulsive regime widens. Note that we only consider $g(t) \leq g_c$ for a simplicity [32–34].

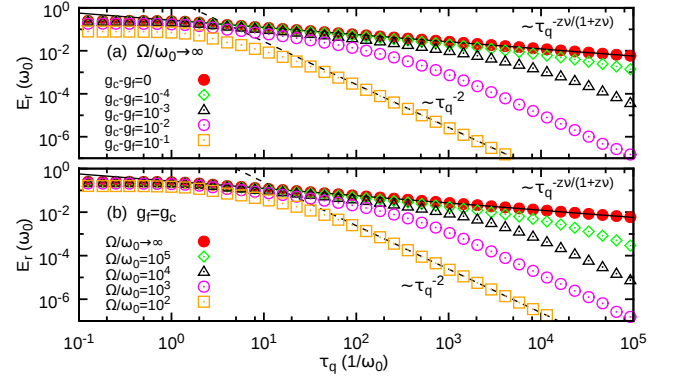


FIG. 2. Residual energy E_r as a function of the quench time τ_q obtained by solving a nearly adiabatic dynamics for (a) different values of the final coupling strength g_f ranging from $g_f = 0.9g_c$ to $g_f = g_c$ (from bottom to top) in the $\Omega/\omega_0 \rightarrow \infty$ limit and (b) different ratios Ω/ω_0 ranging from $\Omega/\omega_0 = 10^2$ to $\Omega/\omega_0 \rightarrow \infty$ (from bottom to top) with a fixed final coupling strength $g_f = g_c$. For $g_f = g_c$ in the $\Omega/\omega_0 \rightarrow \infty$ limit, it precisely follows the universal scaling relation (solid line), predicted by the Kibble-Zurek mechanism. Both moving g_f away from g_c and reducing the ratio Ω/ω_0 result in a crossover from the universal scaling to τ_q^{-2} scaling (dashed line).

The wave function at time t can be expressed in terms of the instantaneous eigenstates of $H_{np}(g(t))$, i.e., $|\Psi(t)\rangle = \sum_m c_m(t)\mathcal{S}[r_{np}(t)]|m\rangle$. Then, we apply the adiabatic perturbation theory [9, 32, 34] to calculate the residual energy E_r at the end of the quench, which measures the degree of non-adiabaticity, defined as $E_r \equiv \langle \Psi(\tau_q) | H_{np}(g(\tau_q)) | \Psi(\tau_q) \rangle - E_G(g(\tau_q))$. For a protocol that stays in the adiabatic regime, i.e., $g_f \ll \hat{g}$, we obtain a scaling relation, $E_r \propto \tau_q^{-2}$ [39], which is a typical scaling for the adiabatic dynamics with a finite quench time for a gapped Hamiltonian. If the protocol involves the impulsive regime, $g_f \sim \hat{g}$, we find that the residual energy follows a universal scaling relation,

$$E_r \propto \tau_q^{-z\nu/(z\nu+1)}, \quad (7)$$

that is, $E_r \propto \tau_q^{-1/3}$ since $z\nu = 1/2$ [39]. A different way to predict the universal scaling of E_r based on KZM is to use the dynamical scaling function approach [17], which expresses the scaling relation in terms of the finite-frequency scaling exponents. We confirm that it predicts the same universal scaling relation as in Eq. (7) [39].

For short-range interaction models, the residual energy due to a slow quench stems from spatial defects in order parameter across a QPT, whose scaling has been successfully predicted by KZM [7, 10, 11]. However, it is not clear whether KZM can predict the scaling of the residual energy in fully-connected models due to their lack of spatial degrees of freedom. In fact, although the same scaling relation with Eq. (7) has also been predicted for the Dicke and LMG model [17], a numerical calculation with a finite-size LMG model shows a significant discrepancy with the universal scaling as it estimates $E_r \propto \tau_q^{-3/2}$ [16], raising a doubt on the applicability of

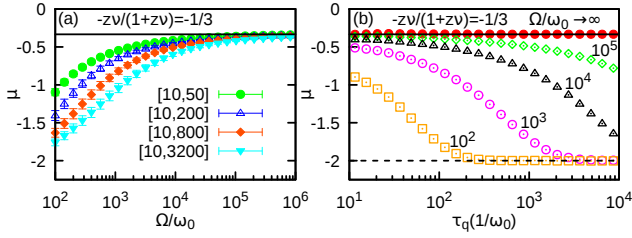


FIG. 3. Exponents of power-law scaling τ_q^μ for the residual energy E_r presented in Fig. 2 (b). (a) Fits obtained for different ranges of the quench time $[\tau_{q1}, \tau_{q2}]$. The values for $\tau_{q1(q2)}$ are indicated in the figure. The exponent μ converges to the universal scaling exponent $-1/3$ for finite Ω/ω_0 . (b) Fits obtained for a range of the quench time $[\tau_q \Delta\tau_q, \tau_q/\Delta\tau_q]$ as a function of τ_q with a fixed log-scale interval $\log_{10} \Delta\tau_q = 6.25 \times 10^{-2}$. The crossover from $\mu = -2$ to $\mu = -1/3$ as one increases Ω/ω_0 is clearly demonstrated.

the KZM to the fully-connected models [17]. Strictly speaking, one has to solve the dynamics exactly in the thermodynamic limit for the LMG or Dicke model, or equivalently in the $\Omega/\omega_0 \rightarrow \infty$ limit for the Rabi model to test the validity of the universal scaling relation, which is accomplished in the following section.

Exact solution for adiabatic dynamics.— The exact low-energy effective Hamiltonian given in Eq. (2) allows one to numerically solve the slow quench dynamics of the Rabi model, which involves only a small number of quasiparticle excitations, in the $\Omega/\omega_0 \rightarrow \infty$ limit. The equation of motion is given as $i\dot{a}_H(t) = [a_H(t), H_{np,H}(t)]$, where the subscript H indicates the operators in the Heisenberg picture. We express the cavity field operator at time t as $a_H(t) = u(t)a(0) + v^*(t)a^\dagger(0)$ with an initial condition $u(0) = 1$ and $v(0) = 0$, and $|u(t)|^2 - |v(t)|^2 = 1$, and derive coupled differential equations for $u(t)$ and $v(t)$,

$$\begin{aligned} \frac{i}{\omega_0} \frac{du(t)}{dt} &= \left(1 - \frac{g^2(t)}{2}\right) u(t) - \frac{g^2(t)}{2} v(t), \\ -\frac{i}{\omega_0} \frac{dv(t)}{dt} &= \left(1 - \frac{g^2(t)}{2}\right) v(t) - \frac{g^2(t)}{2} u(t). \end{aligned} \quad (8)$$

The residual energy in terms of $u(t)$ and $v(t)$ is given by

$$E_r = \omega_0 |v(t)|^2 - \frac{\omega_0 g_f^2}{4} |u(t) + v(t)|^2 - \frac{\epsilon_{np}(g_f) - \omega_0}{2}. \quad (9)$$

In Fig. 2 (a), we plot E_r at the end of the quench as a function of τ_q for different values of the final coupling strength g_f in the $\Omega/\omega_0 \rightarrow \infty$ limit. For a protocol that ends right at the critical point, $g_f = g_c$, it precisely follows the universal scaling given in Eq. (7). It confirms that the nearly adiabatic dynamics of the QPT in the Rabi model can be completely characterized by the critical exponents alone, thus is universal, and that the KZM can be successfully applied to a fully-connected model. We note that the saturation of E_r observed for a short quench

time, $\tau_q \lesssim 1/\omega_0$, corresponds to sudden quench dynamics. As we change g_f progressively away from the critical point, $g_f < g_c$, the universal scaling breaks down and the τ_q^{-2} scaling emerges, which is precisely the scaling predicted using the adiabatic perturbation theory in the adiabatic regime [39].

We find that the leading order correction to the equation of motion for finite Ω/ω_0 adds an additional term, $f(u, v) = (3\omega_0/4\Omega)g^4(t)(u+v)|u+v|^2$, to the right hand side of both equations in Eq. (8) [39]. For a quench that ends at the critical point $g_f = g_c$, the leading order correction to the residual energy adds an additional term, $h(u, v) = (3\omega_0^2 g_c^4)/(16\Omega)|u+v|^4 - \frac{\omega_0}{4}(2\Omega/3\omega_0)^{-1/3}$, to Eq. (9) [39]. In Fig. 2 (b), where we reduce the ratio Ω/ω_0 from infinity to 10^2 for $g_f = g_c$, we observe a crossover behavior for the residual energy virtually identical to Fig. 2 (a). This is because a finite value of Ω/ω_0 opens up an energy gap at $g_f = g_c$ whose effect is equivalent to ending the protocol away from the critical point.

An interesting aspect of the crossover behavior for the scaling of E_r shown in Fig. 2 (b) is that there is a range of quench time τ_q at around $\tau_q \in [10, 10^3]$ where the E_r closely follows the universal power-law even for finite values of Ω/ω_0 . By closer inspection, we find fits for the slope of curves in Fig. 2 (b), which corresponds to the exponents of power-law scaling of E_r , for a wide range of quench times. As shown in Fig. 3 (a), the exponents converge to the universal scaling exponent $-1/3$ as one increases the ratio Ω/ω_0 , showing that the onset of the universal dynamics can be observed with finite Ω/ω_0 . The convergence to the universal scaling implies that the energy gap whose scaling is given in Eq. (6) is sufficiently small to drive the system into the impulsive regime so that the dynamics is strongly influenced by the nature of the critical point. As the energy gap widens for smaller values of Ω/ω_0 , the influence of the critical points gradually vanishes, leading to a crossover to τ_q^{-2} scaling. In Fig. 3 (b), the crossover of the scaling from $\tau_q^{-1/3}$ to τ_q^{-2} is further elucidated by finding fits for much shorter interval of τ_q , which approximates the slope of the tangent line of graphs in Fig. 3 (b). Varying g_f in the $\Omega/\omega_0 \rightarrow \infty$ limit shows identical features shown in Fig. 3 [39].

Conclusion.— We have found an effective low-energy description of the Rabi model that unveils the universality of the model both in and out of equilibrium. Our analysis shows that the superradiant QPT which has been primarily studied for systems of thermodynamically many atoms can as well be investigated with systems of a single atom. An important advantage of the reduced degrees of freedom is that solving the critical dynamics is more tractable; indeed, we have been able to report a first confirmation of the KZM prediction for a fully-connected model. Together with an impressive ongoing progress of technologies to realize the interaction between a two-level system and a single harmonic oscillator, we expect that the Rabi model can serve as an excellent platform to study equilibrium and non-equilibrium critical phenomena.

Acknowledgements.— This work was supported by the EU Integrating projects SIQS and DIADEMS, the EU STREP

-
- [1] S. Sachdev, *Quantum Phase Transitions*, 2nd ed. (Cambridge University Press, 2011).
- [2] A. Polkovnikov, K. Sengupta, A. Silva, and M. Vengalattore, *Reviews of Modern Physics* **83**, 863 (2011).
- [3] J. Eisert, M. Friesdorf, and C. Gogolin, *Nature Physics* **11**, 124 (2015).
- [4] T. W. B. Kibble, *Journal of Physics A: Mathematical and General* **9**, 1387 (1976).
- [5] W. H. Zurek, *Nature* **317**, 505 (1985); *Physics Reports* **276**, 177 (1996).
- [6] P. Laguna and W. Zurek, *Physical Review Letters* **78**, 2519 (1997).
- [7] A. del Campo and W. H. Zurek, *International Journal of Modern Physics A* **29**, 1430018 (2014).
- [8] B. Damski, *Physical Review Letters* **95**, 035701 (2005).
- [9] A. Polkovnikov, *Physical Review B* **72**, 161201 (2005).
- [10] W. Zurek, U. Dorner, and P. Zoller, *Physical Review Letters* **95**, 105701 (2005).
- [11] J. Dziarmaga, *Physical Review Letters* **95**, 245701 (2005); *Advances in Physics* **59**, 1063 (2010).
- [12] G. Nikoghosyan, R. Nigmatullin, and M. B. Plenio, arxiv:1311.1543 (2013).
- [13] R. Botet, R. Jullien, and P. Pfeuty, *Physical Review Letters* **49**, 478 (1982); R. Botet and R. Jullien, *Physical Review B* **28**, 3955 (1983).
- [14] R. H. Dicke, *Phys. Rev.* **93**, 99 (1954).
- [15] H. J. Lipkin, N. Meshkov, and A. J. Glick, *Nuclear Physics* **62**, 188 (1965).
- [16] T. Caneva, R. Fazio, and G. Santoro, *Physical Review B* **78**, 104426 (2008).
- [17] O. L. Acevedo, L. Quiroga, F. J. Rodríguez, and N. F. Johnson, *Physical Review Letters* **112**, 030403 (2014).
- [18] K. Hepp and E. H. Lieb, *Annals of Physics* **76**, 360 (1973).
- [19] Y. Wang and F. Hioe, *Physical Review A* **7**, 831 (1973).
- [20] C. Emary and T. Brandes, *Physical Review Letters* **90**, 044101 (2003).
- [21] C. Emary and T. Brandes, *Physical Review E* **67**, 066203 (2003).
- [22] V. M. Bastidas, C. Emary, B. Regler, and T. Brandes, *Physical Review Letters* **108**, 043003 (2012).
- [23] F. Dimer, B. Estienne, A. Parkins, and H. Carmichael, *Physical Review A* **75**, 013804 (2007).
- [24] K. Baumann, C. Guerlin, F. Brennecke, and T. Esslinger, *Nature* **464**, 1301 (2010).
- [25] K. Baumann, R. Mottl, F. Brennecke, and T. Esslinger, *Physical Review Letters* **107**, 140402 (2011).
- [26] L. Bakemeier, A. Alvermann, and H. Fehske, *Physical Review A* **85**, 043821 (2012).
- [27] G. Levine and V. Muthukumar, *Physical Review B* **69**, 113203 (2004).
- [28] A. Hines, C. Dawson, R. McKenzie, and G. Milburn, *Physical Review A* **70**, 022303 (2004).
- [29] S. Ashhab and F. Nori, *Physical Review A* **81**, 042311 (2010).
- [30] M.-J. Hwang and M.-S. Choi, *Physical Review A* **82**, 025802 (2010).
- [31] S. Ashhab, *Physical Review A* **87**, 013826 (2013).
- [32] C. De Grandi, V. Gritsev, and A. Polkovnikov, *Physical Review B* **81**, 012303 (2010).
- [33] C. De Grandi and A. Polkovnikov, in *Quantum Quenching, Annealing and Computation*, edited by A. K. Chandra, A. Das, and B. K. Chakrabarti (Springer, Heidelberg, 2010).
- [34] C. De Grandi, V. Gritsev, and A. Polkovnikov, *Physical Review B* **81**, 224301 (2010).
- [35] D. Braak, *Physical Review Letters* **107**, 100401 (2011).
- [36] J. Schrieffer and P. Wolff, *Phys. Rev.* **149**, 491 (1966).
- [37] S. Bravyi, D. P. DiVincenzo, and D. Loss, *Annals of Physics* **326**, 2793 (2011).
- [38] The same Hamiltonian was used in Ref. [26] to calculate a quantum correction to a mean-field result for the diverging variance of position quadrature of the cavity field.
- [39] See Supplemental Material at [URL will be inserted by publisher] for further explanation and details of the calculation.
- [40] J. Vidal and S. Dusuel, *Europhysics Letters* **74**, 817 (2006).
- [41] S. Dusuel and J. Vidal, *Physical Review Letters* **93**, 237204 (2004).
- [42] S. Dusuel and J. Vidal, *Physical Review B* **71**, 224420 (2005).